Analysis of Wireless Power Supplies for Industrial Automation Systems

K. O'Brien, G. Scheible*, H. Gueldner

Dresden University of Technology
Department of Electrical Engineering
01062 Dresden, Germany

*ABB Corporate Research
Wallstadter Str. 59
68526 Ladenburg, Germany

Abstract—**Abundant sensors used in non-stationary, maintenance-free industrial environments with high sensor densities are preferably powered by a wireless power system. For most industrial applications this is possible with a magnetic supply principle, based on unconventional transformers with large air-gaps. This paper presents an analytical description of the magnetic components of a wireless power supply system based on the magnetic coupling of multiple spatially separated coils. The power transfer through the large air-gap transformer is accurately predicted using a coupling model.**

I. INTRODUCTION

Novel power supplies for use in applications such as robotics, automated production machines, and applications with high insulation requirements where wired energy transfer is not suitable have recently been proposed [1], [2], [3],[4]. These power supplies together with suitable wireless communication devices eliminate wires and connectors which were identified as one of the major causes of equipment down-time. Alternatives, such as batteries, are not well suited for long-term, reliable operation in high volume applications (e.g. > 10,000 units for >10 years).

Unconventional transformers with large air-gaps are used to supply energy to the load via magnetic fields over distances up to several meters and provide for the wireless supply of power to devices such as sensors, communication devices, or actuators.[1] As an example, Figure 1 depicts the main transformer components being used. Multiple primary coils consisting of one or several coils per plane form an orthogonal system. The secondary coils, each consisting of three coils each wound around one of the three axes of a cube-shaped ferrite core are placed inside the box formed by the primary coil(s). Both the primary and secondary components operate in resonance, which allows power transfer to the load to be optimized.

In order to properly analyze the system, the coupling between each individual primary and secondary must be understood and described. Formulas describing the coupling between all possible coil combinations are presented in this paper, and a transformer equivalent circuit model is used to further explain the operation of the system.

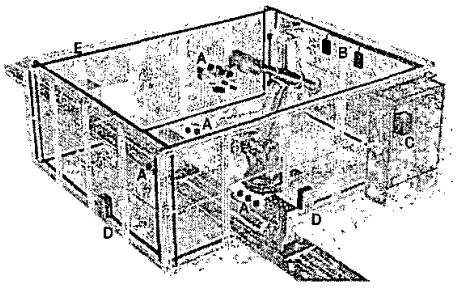

Figure 1 – Example automation application with a robot and a power supply using a large air-gap transformer:
A: Secondary coils (in wireless sensor modules)
B: Communication antenna(s)
C: Wireless I/O module with field bus plug
D: Primary power supplies
E: Primary coil(s)

II. SYSTEM CHARACTERIZATION

The coils can be represented as a system of loosely coupled inductors with the self-inductances L_{pp} and L_{ss} of each coil coupled with each other coil by k_{pxsy}, k_{pxpy}, and/or k_{xxsy} (where p represents a primary coil, s represents a secondary coil, and x and y represent the x^{th} and y^{th} coil). However, each time that a coil is moved the entire set of coupling factors relating to that coil must be recalculated. The system becomes extremely complicated as the number of elements is increased. The number of coupling factors N_k that must be calculated is given by

$$N_k = C_P C_S + C_P + C_S + \frac{C_S!}{2(C_S - 2)!} \qquad (1)$$

where C_S is the number of secondary coils and C_P is the number of primary coils in the system.

Figure 2 shows a system with two primary coils and three secondary coils. Note that although each secondary shown in Figure 2 is actually comprised of three coils wrapped around a ferrite core, these coils are 90 degrees apart spatially and therefore are not coupled to each other in the ideal case.

[1] Patents pending

0-7803-7906-3/03/$17.00 ©2003 IEEE.

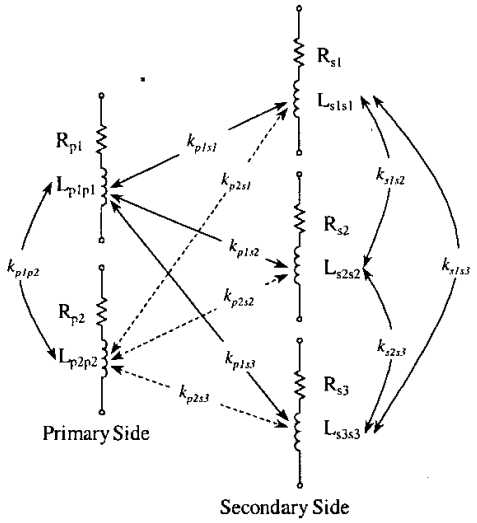

Figure 2 - Coupling between primary and secondary coils

Although prototypes show coupling between these three coils of up to 0.6%, this does not cause significant problems in normal operation of the system. These three coils allow the load to receive constant power regardless of the orientation of the secondary with respect to the primary coil or coils. For the purpose of this analysis, coupling between coils on one secondary will be neglected. The term "secondary coil" will refer to one ferrite cube with one coil wrapped around each of its axes.

Figure 2 can be simplified by ignoring the coupling between secondary coils that are not located within a few centimeters of each other as the coupling between cube shaped secondary coils separated spatially by a distance greater than the value of one side-length of the ferrite core has been seen in preliminary tests and simulations to have a negligible effect on the overall performance of the system.

A. Calculation of Coil Self Inductances

All primary and all secondary coils are of rectangular shape. Other coil shapes were discussed in [4]. The self-inductance of a coil that is comprised of straight elements can be described by the sum of the self-inductance of each straight wire and the mutual inductances of all of the possible wire pairs.

Starting with the differential form of the Biot-Savart Law, [5] approximates the self-inductance of a straight round conductor as

$$L_s \approx 0.2l\left[\ln\frac{2l}{\rho}-\frac{3}{4}\right] \qquad (2)$$

where ρ is the radius and l is the length of the conductor.

The mutual inductance between opposite sides of a rectangular coil (parallel conductors of the same length) is given by [5] as

$$L_{mutual} \approx 0.2l\left[\ln\left(\frac{l}{d}+\sqrt{1+\frac{l^2}{d^2}}\right)-\sqrt{1+\frac{d^2}{l^2}}+\frac{d}{l}\right] \qquad (3)$$

where l is the length of the conductor and d is the distance between the parallel conductors. In this case the radius of the wires can be neglected, as it is very small relative to d [5].

The mutual inductance of two conductors meeting at a right angle is zero. For the purposes of this calculation, the wires forming the primary coils are assumed to form an ideal rectangular system.

Summing the self-inductance (given by (2)) of each of the four wires and the mutual inductances (given by (3)) between each of the possible wire pairs, the self-inductance of a rectangular coil can be described by

$$L_{self} \approx 0.4N^2\left[\begin{array}{l} l\ln\frac{2l}{\rho}+w\ln\frac{2w}{\rho}+2\sqrt{l^2+w^2} \\ -l\sinh^{-1}\frac{l}{w}-w\sinh^{-1}\frac{w}{l} \\ -2(l+w)+\frac{1}{4}(l+w) \end{array}\right] \qquad (4)$$

where l and w are the lengths of the sides of the rectangle, and N is the number of turns in the coil.

Effects of flux concentration due to the presence of a ferromagnetic material: Equation (4) provides a good approximation of the inductance of the primary coils (within approximately 1.5%). While the secondary coils are also rectangular in shape, they are wrapped around a ferrite core. The inherent high initial permeability of the core provides a low reluctance path for the flux created by the primary coils, thereby concentrating the flux lines within the core and increasing the density of the magnetic field. A concentration of flux in the core (when the core material has $\mu_r>1$) will increase the inductance of the coil wrapped around that core. Equation (4) is multiplied by a flux concentration or demagnetisation factor D, which accounts for this effect. This factor is based on the permeability of the core material and on the geometry of the core. Although the exact value of D is extremely difficult to calculate, [6] shows that D for prisms with two sides of equal length can be approximated using the value of D for a cylinder. The demagnetisation factors of cylinders are well known. Reference [7] shows that for cylinders having long and short axes of equal length (a good approximation of the ferrite cube used in this system) and a relative permeability in the range of a few thousands, D is approximately equal to 3.

The effective permeability of the core is then described by [5] as

$$\frac{1}{\mu} = \frac{1}{\mu'} - \frac{N}{4\pi} \tag{5}$$

where μ is the true permeability of the core material and μ' is the effective permeability of the core material.

B. Calculation of Mutual Inductances

The mutual inductance between coils in the system can be found using the Neumann formula for mutual inductance

$$L_{12} = \frac{\mu_0}{4\pi} \oint\oint \frac{d\vec{l}_1 \cdot d\vec{l}_2}{|\vec{r}_2 - \vec{r}_1|} \tag{6}$$

Alternatively, the mutual inductance, L_{ps}, between one primary and one secondary coil can be calculated by integrating the flux density $\vec{B}_P$ created when current passes through the primary coil over the surface S_2 bounded by the secondary coil (Figure 3). This method is made simpler because the flux density at the secondary can be assumed constant over the small area bounded by the secondary coil.

The field density generated by a rectangular coil lying in the y-z plane (where wires 1 and 2 are parallel to the z-axis and wires 3 and 4 are parallel to the y-axis) at any point in the system is shown in [4] to be

$$\begin{aligned}\vec{B}_p = {} & \hat{a}_x N\mu_0 \left(-\sin\phi_1 \frac{IL_1}{2\pi r_1 \sqrt{L_1^2 + r_1^2}} + \sin\phi_2 \frac{IL_2}{2\pi r_2 \sqrt{L_2^2 + r_2^2}} \right. \\ & \left. - \cos\phi_3 \frac{IL_3}{2\pi r_3 \sqrt{L_3^2 + r_3^2}} + \cos\phi_4 \frac{IL_4}{2\pi r_4 \sqrt{L_4^2 + r_4^2}} \right) \\ & + \hat{a}_y N\mu_0 \left(\cos\phi_1 \frac{IL_1}{2\pi r_1 \sqrt{L_1^2 + r_1^2}} - \cos\phi_2 \frac{IL_2}{2\pi r_2 \sqrt{L_2^2 + r_2^2}} \right) \\ & + \hat{a}_z N\mu_0 \left(\sin\phi_3 \frac{IL_3}{2\pi r_3 \sqrt{L_3^2 + r_3^2}} - \sin\phi_4 \frac{IL_4}{2\pi r_4 \sqrt{L_4^2 + r_4^2}} \right)\end{aligned} \tag{7}$$

where $L_{1...4}$ are one half the lengths of each of the four sides of the rectangle, N is the number of turns in the coil, I is the current in the wire, r is the perpendicular distance between the point at which the field is being calculated and the current carrying wire, and ϕ is the angle between the imaginary line of length r connecting the field point with the wire and the x-axis.

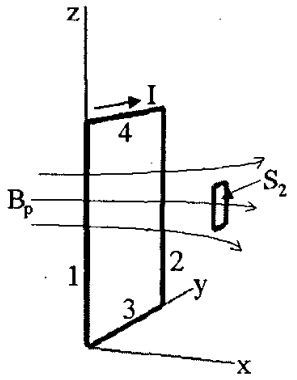

Figure 3 - Flux density B_p passing through the surface S_2 bounded by the secondary coil

Integrating (7) over the surface of the secondary coil to find the flux linking the secondary and assuming that the field is uniform over the surface bounded by the secondary coil

$$\Psi_{ps} = D \int_{S_S} \vec{B}_p \cdot d\vec{s}_S \tag{8}$$

where the subscripts p and s refer to the primary and to the secondary coils, respectively, gives

$$\Psi_{ps} = DA_S\mu_0 |\vec{B}_p| \tag{9}$$

where A_S is the area encompassed by a secondary coil.

Flux linkage Λ_{ps} is defined as

$$\Lambda_{ps} = N_S \Psi_{ps} \tag{10}$$

where N_S is the number of turns on the secondary.

Finally, the mutual inductance between the primary and secondary coils is

$$L_{ps} = \frac{\Lambda_{ps}}{I_p} \tag{11}$$

where I_p is the current in the primary.

The mutual inductance between primary and secondary coils is obviously highly dependent on the position of the secondary coil in question. The mutual inductance between one primary and one secondary coil is found by combining (8), (9), (10) and (11) and simplifying

$$L_{ps} = DN_p N_s A_s \mu_0 \left[\begin{array}{l} \cos\alpha_x \left(-\sin\phi_1 \dfrac{L_1}{2\pi r_1 \sqrt{L_1^2 + r_1^2}} + \sin\phi_2 \dfrac{L_2}{2\pi r_2 \sqrt{L_2^2 + r_2^2}} \right. \\ \left. -\cos\phi_3 \dfrac{L_3}{2\pi r_3 \sqrt{L_3^2 + r_3^2}} + \cos\phi_4 \dfrac{L_4}{2\pi r_4 \sqrt{L_4^2 + r_4^2}} \right) \\ +\cos\alpha_y \left(\cos\phi_1 \dfrac{L_1}{2\pi r_1 \sqrt{L_1^2 + r_1^2}} - \cos\phi_2 \dfrac{L_2}{2\pi r_2 \sqrt{L_2^2 + r_2^2}} \right) \\ +\cos\alpha_z \left(\sin\phi_3 \dfrac{L_3}{2\pi r_3 \sqrt{L_3^2 + r_3^2}} - \sin\phi_4 \dfrac{L_4}{2\pi r_4 \sqrt{L_4^2 + r_4^2}} \right) \end{array} \right] \quad (12)$$

C. Calculation of coupling factors

The coupling factor k_{ps} between the primary and secondary coils is defined as

$$k_{ps} = \frac{L_{ps}}{\sqrt{L_{pp} L_{ss}}} \quad (13)$$

where L_{pp} and L_{ss} are the self-inductances of the primary and secondary coils and L_{ps} is the mutual inductance between the primary and secondary coils.

Substituting (4) and (12) into (13) gives an expression for the coupling factor between the primary and secondary coil which is obviously quite cumbersome. Some simplifications can be made to make the equation easier to use.

D. Simplifications and approximations of inductance and coupling factor calculations

For primary coils of square shape equation (4) describing the self-inductance of rectangular coils can be simplified. The inductance of a square coil where s is the length of one side of the coil is approximated by [5] as

$$L \approx 0.8 s N^2 \left[\ln\left(\frac{s}{\rho}\right) - 0.5240 \right] \quad (14)$$

If the secondary is assumed to be near to the axis of a square primary coil, (12) can be approximated by

$$L_{ps} \approx DN_s N_p A_s \mu_0 4 \cdot \left(-\sin\left(\frac{\pi}{4}\right) \frac{L}{2\pi r \sqrt{L^2 + r^2}} \right) \quad (15)$$

where L is the length of one side of the coil.

The error in (15) increases as the secondary is moved further off axis. The error is proportional to the difference between the field intensity at the actual position of the secondary coil and the field intensity at the position on the axis of the primary coil that is closest to the actual position of the secondary coil. The volume in which this approximation is accurate can be found using methods for finding the volume of a certain field strength [4].

Substituting (14) and (15) into (13) gives an approximation of the coupling factor.

Although the coupling factor k_{ps} between the primary and secondary coils is of central importance, an accurate representation of the system will also include coupling factors between the primary coils, k_{pp}, and between the secondary coils, k_{ss}.

The mutual inductance between two primary coils can be found using the Neumann Formula. Assuming that the primary coils are square loops both of side length a, separated by a distance d on the same axis

$$L_{p1p2} = \frac{2\mu_0}{\pi} \left[\begin{array}{l} a \ln\left(\dfrac{a^2 + \sqrt{a^2 + d^2}}{d} \right) - \sqrt{a^2 + d^2} \\ +d - a \ln\left(\dfrac{a^2 + \sqrt{2a^2 + d^2}}{\sqrt{a^2 + d^2}} \right) \\ +\sqrt{2a^2 + d^2} - \sqrt{a^2 + d^2} \end{array} \right] \quad (16)$$

The coupling factor between two primary coils can then be approximated by substituting (4) and (16) into (13).

Primary coil systems generally consist of sets of coils placed at 90 degrees of spatial separation. If the ideal case (exactly 90 degrees of separation) is assumed, coupling between coils must be calculated only between coils lying on the same axis, as coils separated by 90 degrees have zero coupling between them.

Although flux density can normally be considered constant over the relatively small area bounded by the secondary coil, this is not the case when two secondary coils are placed in close proximity to each other. As the case of two secondary coils coming into close proximity is the main reason for studying the coupling between them, this problem cannot be neglected. A method of numerical integration of the Neumann formula can also be used to find the coupling factor between two secondary coils, taking into account the angle at which the axes of each secondary coil intersects with the axis of the other.

III. SYSTEM MODELLING

Now that L_{pp}, L_{ss}, k_{ps}, k_{pxpy}, and k_{sxsy} have been found, the coils can be represented as a system of coupled inductors with the self-inductances L_{pp} and L_{ss} of each coil coupled with each other coil by k_{ps}, k_{pxpy}, and/or k_{sxsy} as shown in Figure 2. In order to integrate the coupled inductors in a full system description and to allow for a system optimisation, an equivalent circuit was developed.

A classic single-phase equivalent transformer model can be used to represent the energy transfer between one primary and one secondary coil in a wireless power system.

A wireless power system with its inherent large air-gap is characterized by a small magnetizing inductance and large leakage inductances. The core loss resistance, r_c, can be neglected as the core losses are small enough to be considered negligible for the core selected in this case.

The conventional transformer model can be simplified and applied to the wireless power system by referring all values to the secondary side of the transformer and replacing the primary voltage, leakage inductance, and resistance with an ideal current source representing the current flowing in the primary coils. The equivalent circuit model extended by the resonant capacitor, rectifier, dc-filter, and load, is shown in Figure 4.

Winding resistances can be calculated with conventional equations using wire diameter, copper characteristics, number of turns, and the dimensions of the system, taking into account the skin and proximity effects.

Figure 5 shows simulation results using the model shown in Figure 4 for several values of load resistance. Figure 6 shows the current in the primary coil, the magnetic field at the position of the secondary coil, and the dc side voltage for a load of 2kΩ. The simulation model and the practical results confirm the fact that the power available to the load is highly dependant on the coupling between the primary and secondary coils. Figures 7 show the test set-up used in obtaining Figure 6.

Only one set of primary coils was energized during this test and the secondary was aligned along the same axis so that voltage was induced on only one of the coils comprising the secondary. For the multi-dimensional systems used in practical set-ups, Figure 4 must be expanded into a multi-winding transformer model.

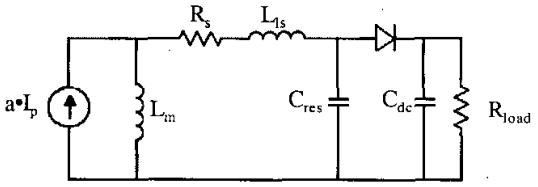

Figure 4 – Simplified equivalent transformer model where

L_m = mutual inductance
R_s = secondary side winding resistance
L_{ls} = secondary side leakage inductance
C_{res} = Secondary side resonant capacitance
C_{dc} = dc-side capacitance
I_p = Primary side current
a = Turns ratio (N_1/N_2).
R_{load} = Load resistance

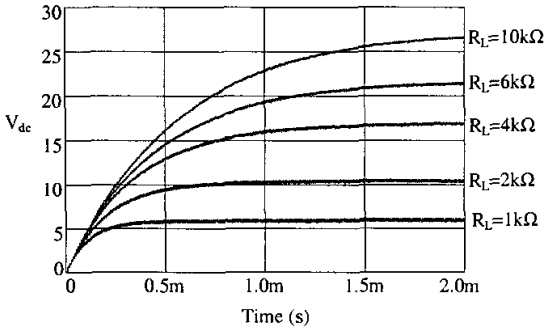

Figure 5 – Simulation results showing rectified secondary voltage for a range of load values

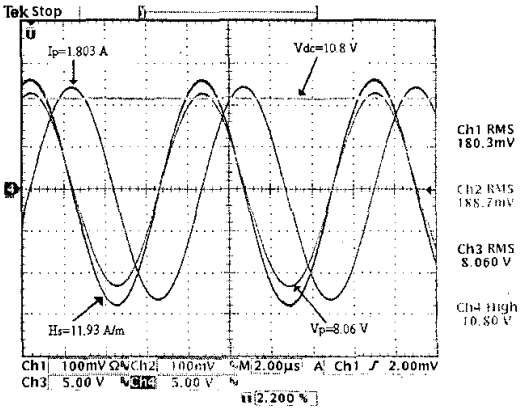

Figure 6 – Primary terminal voltage (V_p), primary current(I_p), magnetic field intensity at secondary coil position (H_s), dc voltage (V_{dc}) at R_L=2kΩ.

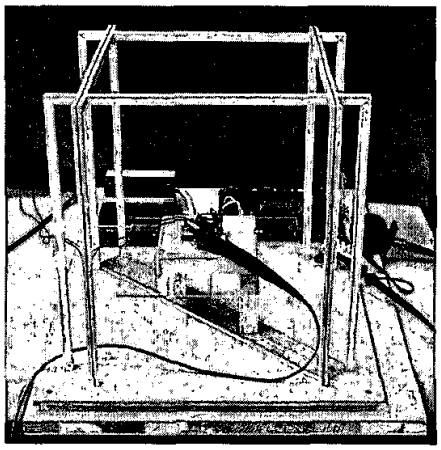

Figure 7 – Test set-up using one secondary coil and square primary coils of 30 cm on each side.

DOCKET ALARM

Explore Litigation Insights

Docket Alarm provides insights to develop a more informed litigation strategy and the peace of mind of knowing you're on top of things.

Real-Time Litigation Alerts

Keep your litigation team up-to-date with **real-time alerts** and advanced team management tools built for the enterprise, all while greatly reducing PACER spend.

Our comprehensive service means we can handle Federal, State, and Administrative courts across the country.

Advanced Docket Research

With over 230 million records, Docket Alarm's cloud-native docket research platform finds what other services can't. Coverage includes Federal, State, plus PTAB, TTAB, ITC and NLRB decisions, all in one place.

Identify arguments that have been successful in the past with full text, pinpoint searching. Link to case law cited within any court document via Fastcase.

Analytics At Your Fingertips

Learn what happened the last time a particular judge, opposing counsel or company faced cases similar to yours.

Advanced out-of-the-box PTAB and TTAB analytics are always at your fingertips.

API

Docket Alarm offers a powerful API (application programming interface) to developers that want to integrate case filings into their apps.

LAW FIRMS
Build custom dashboards for your attorneys and clients with live data direct from the court.

Automate many repetitive legal tasks like conflict checks, document management, and marketing.

FINANCIAL INSTITUTIONS
Litigation and bankruptcy checks for companies and debtors.

E-DISCOVERY AND LEGAL VENDORS
Sync your system to PACER to automate legal marketing.